Astronomical and Astrophysical Transactions (*AApTr*), 2020, Vol. 31, Issue 4, pp. 473–492,
ISSN 1055-6796, Photocopying permitted by license only, ©Cambridge Scientific Publishers

Study of variability of 3C 144 (Taurus A) radio source at frequencies 1.6, 5, 6.1 GHz with passage through the Solar supercorona

A. Sukharev[1,2,*], M. Ryabov[2], L. Sobitniak[2], V. Bezrukovs[1], A. Orbidans[1], M. Bleiders[1], S. Panishko[2]

[1] *Ventspils International Radio Astronomy Centre of the Ventspils University College Institute of Engineering, Inzenieru str. 101, Ventspils, LV-3601, Latvia*
[2] *Institute of Radio Astronomy of the National Academy of Sciences of Ukraine, Mystetstv str. 4, Kharkiv, 61022, Ukraine*

Received 1 October, 2019

The galactic radio source 3C 144 (identified with the Crab Nebula) is one of the most important objects for studying the structure of the solar wind. Being in ecliptic plane and approaching minimum distance to the Sun on June 15 every year, 3C 144 shines through the Solar supercorona, which is observed (usually at meter and decameter wavelengths) in the form of radio emission scintillations on inhomogeneities of the solar wind. This paper presents preliminary results of the study of variability of 3C 144 (in May, July 2019) at frequencies 1.6, 5, 6.1 GHz at the 32-m radio telescope of the Ventspils International Radio Astronomy Center in Latvia. A possible relationship between active events on the Sun, which caused disturbances in the solar wind and observed flux density variability, is shown. Characteristic times of variability, observed at 1.6 GHz, are from several hours to 20 minutes; at frequencies of 5 and 6.1 GHz, from 2–3 hours to 40–30 minutes. Also, fast variations of solar wind parameters (proton density, plasma pressure, wind speed, plasma temperature) were analyzed using satellite data from the NASA OmniWeb catalog, with hourly, five minute and one minute averaging. Using the method of continuous wavelet analysis, it was shown that quasi-periods in variations of 3C 144 flux density, in band from 10 to 3 hours and from 2 hours to 20 minutes, are close to corresponding quasi-periods in variations of the solar wind parameters. Additionally, variations of 3C 144 flux density were analyzed according to the monitoring program on the "URAN-4" radio telescope at the Odessa Observatory of the RI NASU (frequency 25 MHz, decameter wavelength range). Changes in flux of this radio source at decameter waves depend on the time of culmination. For day and evening observations, a response of its flux to the extreme appearance of solar and geomagnetic activity is noted. For night observations, changes in radio source flux correlate with solar wind parameters. Thus, combination studies of radio source 3C 144 in centimeter, decimeter and decameter wavelengths range complement each other. They make it possible to identify effects of the appearance of variability of the radio

*Email: artem.sukharev@venta.lv

source itself, the influence of inhomogeneities in solar wind and contribution of the ionosphere as a response to active events on the Sun.

Keywords: Taurus A, solar wind, radio telescope, antenna array, radio variability

1 Introduction

The galactic radio source 3C 144 (Taurus A) identified with the Crab nebula (remnant of supernova SN1054) is one of the most important objects for studying the structure of the solar wind. A feature of this radio source is its location in ecliptic plane and every year, in June, 3C 144 "passes" through the region of the Sun's supercorona, reaching minimum angular distance from the Sun on June 15. Characteristic times of flux density variations during interplanetary scintillations are several seconds or less. At higher frequencies of decimeter and centimeter ranges, the features and properties of the 3C 144 radio emission variations as it approaches to the Sun are much less studied. In this paper, preliminary results are presented of observations (May–July 2019) of fast flux variability of the 3C 144, performed at the 32-m radio telescope of the Ventspils International Radio Astronomy Center (VIRAC) in Latvia, at 1.6 GHz (wavelength 19 cm) and 5, 6.1 GHz (wavelengths 6 and 4.9 centimeters). The aim of this work was to study long-term changes in flux density of 3C 144 with characteristic times from several hours to half an hour and slightly less. Additionally, for comparison, features of radio emission variations in decameter range (at frequency 25 MHz, wavelength 12 meters) are considered according to observations on phased array "URAN-4" (Mayaki village, Odessa region) of the Radio Astronomy Institute of the National Academy of Sciences of Ukraine. At low frequencies of 10–30 MHz, the ionosphere makes the largest contribution to observed variability of radio emission, the state of which in turn depends on active events on the Sun causing magnetic storms on the Earth. Thus, the properties of 3C 144 flux variations at frequency 25 MHz show features of the ionospheric response associated with disturbances in the geomagnetic field caused by variations in the solar wind. To check the possible connection of observed 3C 144 variability in decimeter and centimeter ranges with variations in the main parameters of the solar wind, we analyzed time series of data (with hourly, 5- and 1-minute averaging) of speed, temperature, pressure, and proton concentration of solar wind, for April–July 2019, from the NASA OmniWeb database (https://omniweb.gsfc.nasa.gov/).

2 Brief information about the Crab Nebula

The Crab Nebula – this is one of the most powerful galactic radio sources – is the remnant of supernova, observed by Chinese and Arab astronomers in 1054 AD. The distance to the nebula is 6500 light years, the largest size of the nebula is 11 light years, expansion speed is 1500 km/s, approximate mass is 4.6 solar masses, minimum angular distance achieved when approaching the Sun is 4.5 solar radii. It is a powerful X-ray and gamma source, and the central object of this remnant is the pulsar PSR B0531 + 21, emitting strictly periodic radio pulses (rotation speed 30 turns per second) [1].

According to observations scattering of radio emission from 3C 144 as it approaches the Sun, in 1953, V.V. Vitkevich discovered the super corona of the Sun, about 12–15 solar radii in size (the region of solar wind that has the greatest effect on emission of translucent radio sources). For the first time, the properties of Crab Nebula scattering emission by plasma inhomogeneities of supercorona of the Sun were studied in meter wavelength range at the Crimean station of the P.N. Lebedev Physics Institute [2, 3]. In the X-ray and gamma ranges, emission of the Crab Nebula has a variability (with characteristic time about year, as well as month, and possibly less) and flare activity [4, 5].

3 Radio telescopes and data processing methods

3.1 Radio telescope RT-32 VIRAC

At frequencies 1.6, 5, and 6.1 GHz, observations were performed on the 32-m VIRAC radio telescope (Irbene, Latvia) using uncooled (1.6 GHz) and liquid-helium cooled (5, 6.1, 6.7, 8.4 GHz) full power receivers with SDR registrar, in left (LCP) and right (RCP) circular polarizations. Photo of the radio telescope is shown in Figure 1.

On average, in good, slightly cloudy weather, the number of flux density points was about 200 per day. In June, test observations began with an improved method for obtaining flux density readings, which made it possible to increase the sampling frequency to 3 Hz (three samples per second) at a frequency of 1.6 GHz, and in



Figure 1 32-m VIRAC radio telescope.

July, observations began using this technique at frequencies of 5 and 6.1 GHz. This made it possible to highlight fast flux variations with characteristic times of about 30 minutes or less. Observations with high temporal resolution were carried out in series – one to two hours recording of the studied radio source and then recording of the calibration sources. If there was strong external noise in an observation session, it was immediately recognized by synchronous distortions in flux variations of the studied and calibration sources.

Standard practice for observation on VIRAC antennas is as follows. After pointing the telescope to the source and selecting the frequency at which the flux will be measured, the power of the source is measured on antenna's beam (TP_{scr1}), then measuring the background power in the sky (TP_{sky}), further – the measurement of the background power in the sky with the noise generator turned on (TP_{cal}) and the control measurement of the source power (TP_{scr2}) to reduce the influence of external noise and change the elevation angle of the telescope. The noise generator is calibrated noise diode. Further, to obtain the flux density, the following formulas are used:

$$S_f = \frac{T_{cal}}{DPFU \cdot G(el)} \cdot \frac{TP_{src} - TP_{sky}}{TP_{cal} - TP_{sky}},$$

where $G(el)$ – the gain dependence on the elevation angle of the antenna,

$$DPFU = \frac{T_{sys}}{S_{cal}} \cdot \frac{TP_{src} - TP_{sky}}{TP_{sky}}$$

DPFU (Degree Per Flux Unit) – gain in the form of increment receiver temperature per unit of flux density, K/Jy, S_{cal} – flux density of calibration source in Jy, T_{sys} – antenna temperature in K calculated as

$$T_{sys} = T_{cal} \cdot \frac{TP_{sky}}{TP_{cal} - TP_{sky}}.$$

Thus, every seven samples of flux density obtained were averaged to reduce interference. Since June 2019, the methodology for increasing the sampling frequency to 3 Hz has been tested, and each received count of flux density without averaging was recorded in a log file. The disadvantage of this is a high noise level, which requires subsequent effective data smoothing. More complete information on the calibration and measurements, for example, on a 16-m radio telescope, is described in [6].

3.2 Radio telescope "URAN-4" of the Radio Astronomy Institute NAS of Ukraine

The URAN-4 radio telescope RI NASU is an element of unique low-frequency VLBI (radio interferometer with extra-long base) URAN system located in Ukraine with maximum distance between elements of 1 thousand km. Since its commissioning in 1987, in addition to VLBI observations, the URAN-4 radio telescope has been used in long-term flux monitoring of powerful galactic and extragalactic radio sources. Since 1994, the radio telescope switched to digital recording and automatic control and, in absence of interference, performs daily observations according to pre-made program. The entire monitoring period from 1987 to present time includes registration flux

variations of radio galaxies: 3C 274 (Virgo A), 3C 405 (Cygnus A) and supernova remnants: 3C 144 (Taurus A), 3C 461 (Cassiopeia A). The main operating frequencies are 20 and 25 MHz. Observations of radio sources are carried out in separate sessions passing through beam pattern at different hour angles, within ±2 hours before and after time of their culmination. Travel time of 3C 144 radio source through antenna beam pattern was 40 minutes for each hour angle. As a result of monitoring fluxes of radio sources, observation data were obtained at different times of day under various conditions of solar activity. Observations of radio sources during year were carried out both in daytime and at night, which makes it possible to study scintillations of radio sources in various states of the ionosphere [7].

3.3 Observational data analysis technique

To obtain time-frequency spectra of solar wind parameters, "fast" method of continuous wavelet analysis was used, calculated through FFT [8], by analogy with detailed description of application and properties of wavelet analysis in classical work [9], with analyzing wavelet type Derivative of Gaussian (DOG).

Lomb–Scargle periodograms for non-uniform time series were calculated using "fast" method, through FFT proposed in work [10] which significantly increases the speed of calculations for large data series with length of several thousand or more points. To improve the reliability of maxima in periodograms under conditions of noise and irregular variations of analyzed data, we used the Kaiser–Bessel spectral window with value 4 of smoothing parameter. When analyzing observations of radio sources, it is often not very important to accurately determine exact values of quasiperiods, since irregular variations are present in the data. Therefore, there may be many closely spaced peaks on periodograms. In this case, it is important to find areas consisting of many close frequencies that make the greatest contribution to quasiperiodic behavior in time series of observations. The Kaiser–Bessel spectral window has small side lobes and is well suited for this purpose, but at the cost of reducing frequency resolution [11]. The obtained frequencies of periodogram maxima, their amplitudes and phases were used as initial values in construction of trigonometric polynomials, with the Levenberg–Marquardt iterative method [12]. If quasiperiods are determined correctly, then good agreement is observed between approximating trigonometric polynomial and real observational data.

Data series were smoothed using the moving average method, and before applying digital spectral analysis, the average value was subtracted from the data so that periodograms were not distorted by a very large initial value of a frequency close to zero. To isolate and select individual elements of time series corresponding to the region of interest in the Fourier spectrum, we applied band-pass FFT filtering for pre-interpolated data [13].

4 VIRAC observations

From April 30 to May 21 at frequency 1.6 GHz, 2325 flux density points of radio source 3C 144 were obtained. For comparison, radio galaxy Virgo A (3C 274) and two calibration highly stable radio sources 3C 196 and 3C 286 (Seyfert I type

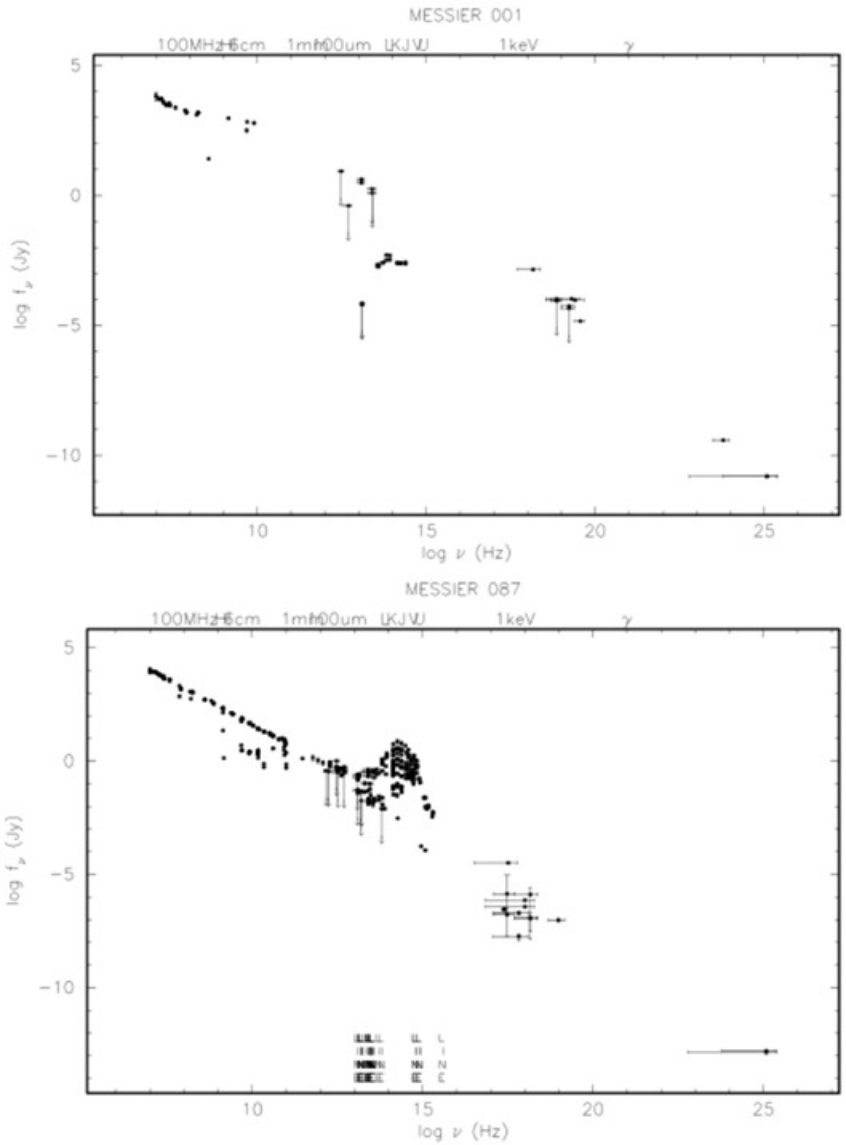


Figure 2 The full (radio-gamma) spectra of radio sources 3C 144 (above) and 3C 274 (below). In radio range, spectra have the form of almost straight lines with decreasing flux density and with increasing frequency (synchrotron emission), which indicates constancy of flux density in a wide frequency range.

galaxies) were observed. In radio range the 3C 144 and 3C 274 are almost constant sources, their full spectra (from the NASA / IPAC Extragalactic Database (http://ned.ipac.caltech.edu/)) are shown in Figure 2. Thus, in flux density variability observed at 1.6 GHz, the contribution of possible intrinsic variability of 3C 144 radio source is negligible.

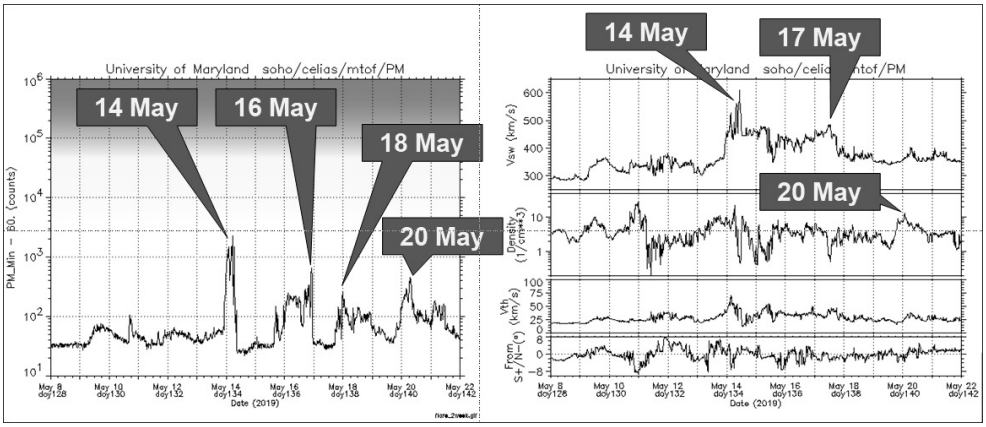


Figure 3 The figure shows days of disturbances in speed, density and energy of solar wind particles, according to the SOHO spacecraft (https://sohowww.nascom.nasa.gov/).

In May 2019, increased geomagnetic activity was observed on the following days: 1–2, 7, 10–11, 13–14, 29. Next, we considered variations in flux density of 3C 144 source on these or near these days. Examples of disturbances in solar wind according to device Proton Monitor Sensor (http://umtof.umd.edu/pm/), mounted on spacecraft SOHO, are shown in Figure 3.

On May 1, 2019, with perturbed geomagnetic field after active events on the Sun, quasiperiodic variability of flux density of 3C 144 source was observed with characteristic times 12.2, 4.7, 2.3–1.9 hours. Trigonometric polynomial, with such periods of sinusoids, inscribed in light curve for this day, showed quite good agreement with observed data. On May 6, 2019, the effect of ultraviolet radiation from a solar flare appeared in observation of shortest variability, with characteristic times about 1 hour and 21 to 18 minutes. During period of increased geomagnetic activity on May 10, characteristic times of flux density variations were 2.5 and 1.3 hours. On May 12, 2019, the day before the magnetic storm, quite rapid variations in flux were observed with characteristic times 1.7–1.2 hours. At the same time, for almost the entire period of May observations, which are very close to harmonic, variations of about 1 hour were observed only on May 3, 2019, mainly in the right circular polarization. In the observation session on May 18–21, 2019, disturbances appeared in the solar wind on May 19–20. Reaction of flux density 3C 144 was in the form of a sharp increase in amplitude and decrease in characteristic time of variations. Subsequently, a sharp drop in amplitude was observed when solar wind parameters returned to calm state (Figure 4). Gaps in the graph are associated with short-term interruptions in observations in connection with the performance of other tasks on the antenna.

At the end of June 2019, 1.6 GHz receiver failed. Further observations of 3C 144 in July continued on cooled full power receiver at frequencies 5, 6.1 GHz. Consider the observations at frequencies 5 and 6.1 GHz made in July 2019. Magnetic storms occurred on the following dates: July 10 – severe storm; July 9, 11, 28 – light storms, 18 and 22 minor geomagnetic disturbances were also observed. On July 23 and 24, the

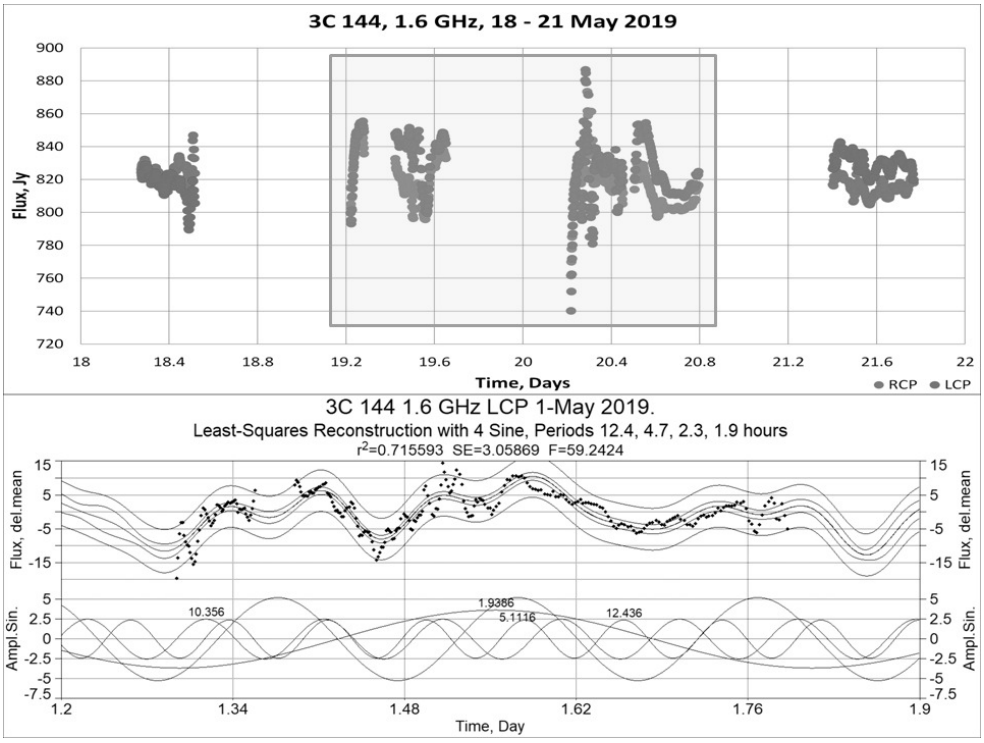


Figure 4 An example (upper panel) of reaction of flux density of source 3C 144, 1.6 GHz to disturbances in solar wind, May 19–20 (indicated by rectangle) in comparison with usual variations in calm wind. An example (bottom panel) of flux density reaction (left circular polarization) after active events that caused geomagnetic disturbances on May 1. Curve of change in flux (point) with subtracted average and also trigonometric approximating polynomial with periods of sinusoids 12.4, 4.7, 2.3, 1.9 hours.

magnetosphere was very calm. However, due to the high load of the 32-m telescope with scientific programs, observations of 3C 144 lasted from July 6 to July 18. On July 10, at frequency 5 GHz, quasiperiod ≈38 minutes (RCP) and ≈37 minutes (LCP) was observed. On July 11, only long-term quasiperiod ≈ 2.4 hours (RCP) and 2.3 hours (RCP) was observed. On July 10, at frequency 6.1 GHz, quasiperiod ≈39 minutes (RCP) and 40 minutes (LCP) was observed. On July 11, at frequency 6.1 GHz, quasiperiod ≈2 hours (RCP) and ≈2.8 hours (LCP) was observed. On July 18, in both polarizations RCP and LCP at frequency 5 GHz, irregular variability was observed, without any quasiperiods. Also on July 18, in contrast to the observations at frequency 5 GHz, at frequency 6.1 GHz quasiperiod about 45 minutes appeared in both circular polarizations. In addition, quasiperiodic variations in flux density at frequencies 5 and 6.1 GHz were observed on July 16. According to SOHO, small splash in speed of solar wind was recorded on this day. For example, initial and smoothed records for 5 GHz (LCP) and 6.1 GHz (RCP) are shown in Figure 5. Values of quasiperiods in variations in flux density for this example are: 33 minutes (5 GHz) and 41 minutes (6.1 GHz).

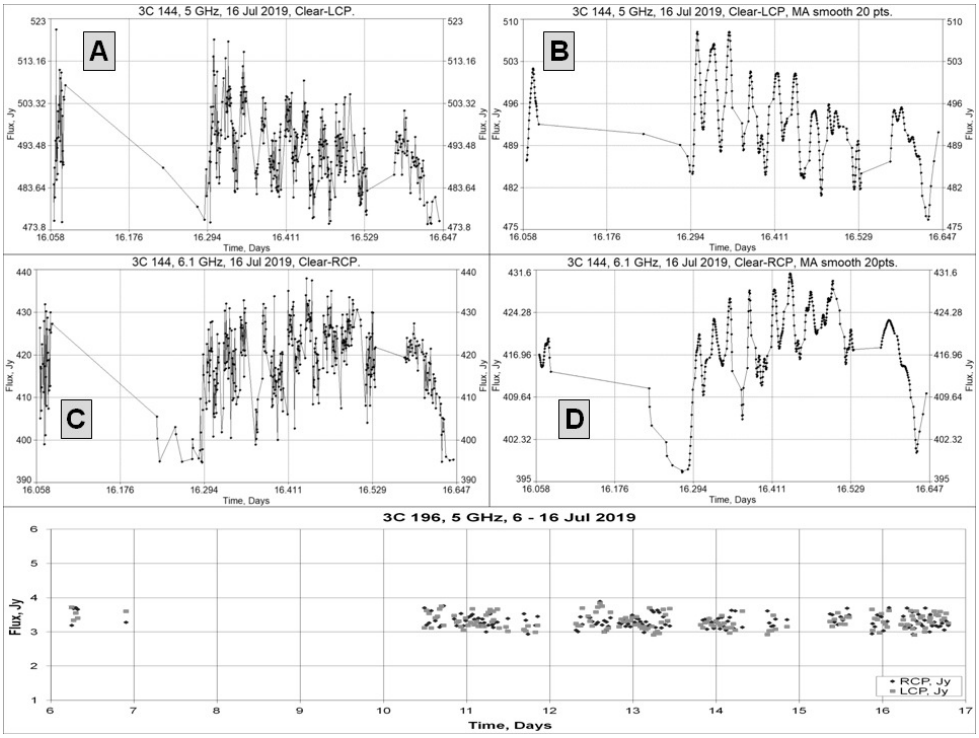


Figure 5 Records of flux density 3C 144 for July 16, 2019. A) 5 GHz, LCP, initial data B) 5 GHz, LCP, smooth data C) 6.1 GHz, RCP, initial data D) 6.1 GHz, RCP, smooth data. Moving average smoothing is performed with window width 20 points. Bottom panel shows recording of standard 3C 196 calibration source at frequency 5 GHz from July 6 to July 16. As can be seen, significant jumps in flux density are not observed.

5 URAN-4 observations

Observations of the 3C 144 radio source on the URAN-4 antenna array were carried out in separate sessions at different hour angles, within ± 2 hours before and after culmination of the sources. Travel time of 3C144 radio source through antenna's beam pattern was 40 minutes for each hour angle. As a result of monitoring fluxes of radio sources, observational data were obtained at different times of day and at different states of solar activity. Changes in fluxes of radio sources at decameter waves are determined by the state of the ionosphere as a result of changes in space weather. In this study, data were taken for 2003, to observe and record the appearance of the most active/high level of solar and geomagnetic activity, which is especially important in conditions when the radio telescope is in the Odessa regional magnetic anomaly, as described in more detail in [14, 15]. Flux of 3C 144 shows the most noticeable increase on October 15, which is observed at all angles hourly. To determine the geomagnetic situation in October 2003, data from the Odessa magnetic observatory (K-index) were used. The Odessa magnetic observatory is located near the URAN-4 radio telescope, which makes it possible to study the geomagnetic activity directly



Figure 6 A) Change in flux level of radio source 3C 144 in October 2003 (25 MHz, polarization A) for different time angles. B) Change in average flux level of radio source 3C 144 relative to K-index. Polarization – A, frequency – 25 MHz (October 2003). C) Change in average flux level of radio source 3C144 relative to the speed of solar wind. Polarization – A, frequency – 25 MHz (October 2003).

in the observation zone. High level of geomagnetic activity on October 14–15 was accompanied by an increase in flux of the radio source. On October 13, the speed of the solar wind gradually increased when a large coronal hole entered the geoeffective position. High-speed flow peaked at about 800 km/s on October 15. Maximum value

of solar wind speed during this active period also led to an increase in the flux level of the radio source (October 15). Flows of electrons with energies above 2 MeV were at a high level on October 16–19. Episodes with increase in flux of the radio source can be associated with the phases of the magnetic storm accompanied by a decrease in electron concentration in the ionosphere leading to a decrease in absorption.

An increase in the growth of electron concentration caused an increase in absorption in the ionosphere and a decrease in the flux level of the radio source. Increase in source flux on October 20–21 is also associated with increased geomagnetic activity according to the Odessa Observatory. After October 25, observations of radio source 3C 144 became exclusively at night (at all angles and times). In this regard, the reaction of flux to an increase in geomagnetic activity was not so significant. There is an increase in flux of 3C 144 source with an increase in solar wind speed. On October 28, one of the largest flares of this solar cycle occurred – proton flare X17 / 4B. Decrease in flux level on October 28–31 is due to absorption in the ionosphere under conditions of increased solar and geomagnetic activity. The corresponding graphs are shown in Figure 6. Thanks to observations of the radio source during day at different angles and at different times/hours, we can see how flux changes during day and from day to day (Figure 6A).

Change in flux level of radio sources is affected not by a single factor, but by a complex of events and processes that form the state of space weather. Therefore, the method of multiple correlation analysis was used in calculations. The 3C144 radio source flux was considered as a dependent variable. The following set of factors were used as independent variables: F10.7 – radio flux at 10.7 cm, Sp – sunspot area, W – Wolf numbers, P – proton flows with energies above 1; 10; 100 MeV, E – electron flows with energies more than 0.6; 2 MeV, density (p) and speed (V) of solar wind in the Earth's orbit (ASE-2), K-index (data from the Odessa magnetic observatory located near the URAN-4 radio telescope are used), main components of geomagnetic field: horizontal component H, vertical component Z, and declination D according to the Odessa magnetic station.

Multiple regression equation was calculated using the least squares method. Selection and calculation of models was carried out taking into account mutual correlation of independent variables, because otherwise, the problem of the estimation of uncertainty arises. At the first stage, the measure of dependence of dependent and independent variables (correlation coefficient) was determined, and then the method of stepwise multiple regression analysis was applied. For example, such characteristics as solar radio emission flux at wavelength 10.7 cm and spots area are interconnected and have high correlation coefficient. Therefore, these indices were introduced into different models for calculating multiple regression. Based on calculations of such models, maximum contributions to the value of multiple correlation coefficient were revealed. Calculation results for models of multiple correlation dependence flux level of the radio source from the indices characterizing the state of space weather are listed in Table 1.

The multiple correlation model shows multiple correlation coefficient 0.88. The largest value of partial correlation coefficient corresponds to index: Np. Corpuscular component, represented by flows of protons and electrons, both during flares and in regular solar wind, also has a noticeable effect on the flux of the radio source. However, proton fluxes with energies > 1 MeV play a leading role here.

Table 1 Summary table, results of calculating multiple regression for radio source 3C 144 (hour angle, 80 min; polarization, A; frequency, 25 MHz) in October 2003. Multiple R, coefficient of multiple correlation.

Multiple R	**0.88**
Proton > 1 MeV	–0.39
Proton > 10 MeV	0.37
Proton > 100 MeV	–0.28
Electron > 0.6 MeV	0.18
Electron > 2 MeV	0.25
Radio flux 10.7 cm	0.33
W	0.31
Sunspot area	0.36
K	–0.34
H	–0.26
Z	0.26
D	0.28
Vspeed [km/s]	–0.18
Np [cm^{-3}]	0.43

6 Analysis of variations in solar wind parameters

If the observed quasiperiodic variations in 3C 144 flux density at decimeter and centimeter radio bands are caused by the passage of radio emission through plasma inhomogeneities of solar wind and correlate with the appearance of solar activity, then quasiperiods close to the observed ones may appear in variations in solar wind parameters (plasma temperature, speed, concentration protons and pressure). To verify this assumption, data from the NASA OmniWeb catalog were taken for April–May 2019 with hourly averaging and additionally for April–July with five-minute, and minute averaging for June 2019. Examples of graphs with hourly averaging are shown in Figure 7. Since the data contains gaps of various durations and are not suitable for wavelet analysis and FFT filtering in their initial form, they were approximated by cubic non-uniform rational B-spline (NURBS) [16] of order 4 (which provides smoother transitions between sharp changes in amplitude in initial data) and which is very resistant to gaps, sharp transitions and outliers in data sets, unlike ordinary cubic splines, which in gaps can produce spurious high-amplitude and false bursts, waves, that can subsequently provide false peaks in periodograms.

Further, using Fourier filtering, spectral regions with periods close to the 3C 144 variability range in decimeter waves were identified, this is most often ≈18–2 hours, and continuous wavelet spectra were calculated. Examples of wavelet spectra for temperature, pressure and plasma speed of solar wind are shown in Figure 8. It can be seen that in these bands of periods there are both quasi-harmonic components with changing periods with time, and components of fast irregular variability, with characteristic times close to observed characteristic times, in variations of flux density 3C 144 for different sessions. Average values of quasiperiods main variations obtained from global wavelet spectra with time averaging (analogue of smoothed Fourier periodogram) for this example: 16, 10.8, 8.8, 4.7 hours (for solar wind temperature) and

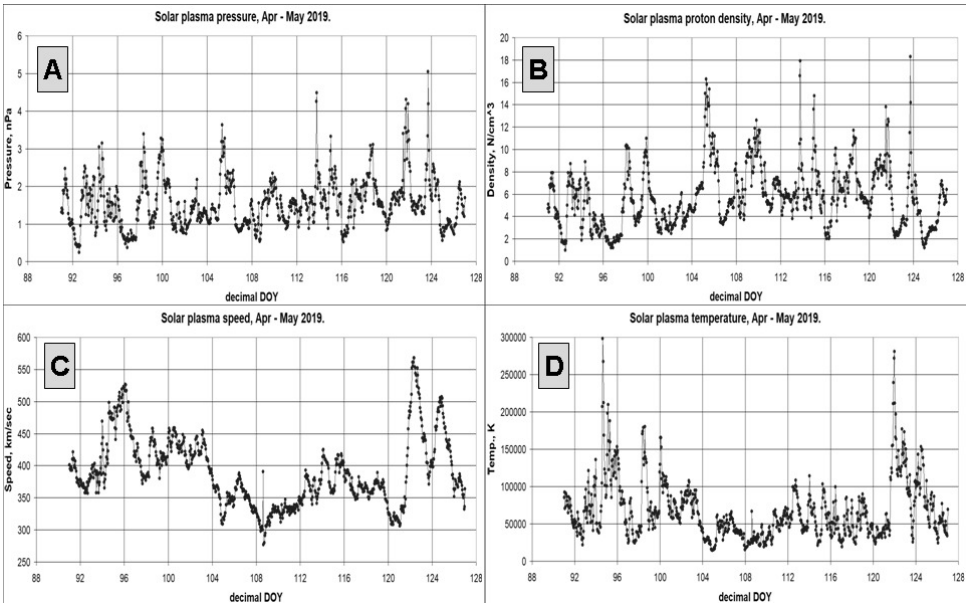


Figure 7 Graphs of some solar wind parameters for April–May 2019 with hourly averaging. A) plasma pressure in nPa; B) Plasma proton density in N/cm^3; C) Wind speed in km/s; D) Plasma temperature in K.

16, 10, 6 hours (for pressure in solar wind) and 16, 12, 9, 7 hours (for solar wind flow speed).

Let us consider variations in solar wind parameters with 5-min averaging for April–July 2019. Data contains rather large gaps, which complicates the use of interpolation even with the use of NURBS splines, since with further use of Fourier filtering a stable false wave appears at points of gaps in the dataset. Therefore, to determine the values of quasiperiods in solar wind parameters, as well as to analyze radio observations, the Lomb–Skargle periodogram was used. For example, for solar wind speed, the main quasiperiods of fast variations (with characteristic time of less than day) were 15.5, 3.4 and 2.3 hours. For the remaining three parameters, the following values of quasiperiods of fast variations were obtained: 14.8, 10.8, 5.8, 1.7 hours (for proton density in solar wind); 15, 10.6, 5.8, 1.7, 1.1 hours (for pressure in solar wind); 17.2, 11.1, 3.1, 1.6 hours (for temperature of solar wind).

Now consider the variations in solar wind parameters (speed, temperature, pressure, proton concentration) for June 2019 with 1-min averaging. In June, there were only occasional test observations on the radio telescope to debug the improved observation technique, since the 32-m antenna was used in EVN (European VLBI Network) session. Therefore, the analysis of solar wind data with minute averaging is done to approximate characteristic times of variations with wind data, 5 min and 1 hour averaging. Since gaps in data were not large, the Akima's classical cubic spline was used for interpolation, which is resistant to insignificant outliers and noise in data and does not produce false waves [17]. Then, FFT filtering removed data components with periods of more than 18 hours in order to remove long-term high-amplitude variations,

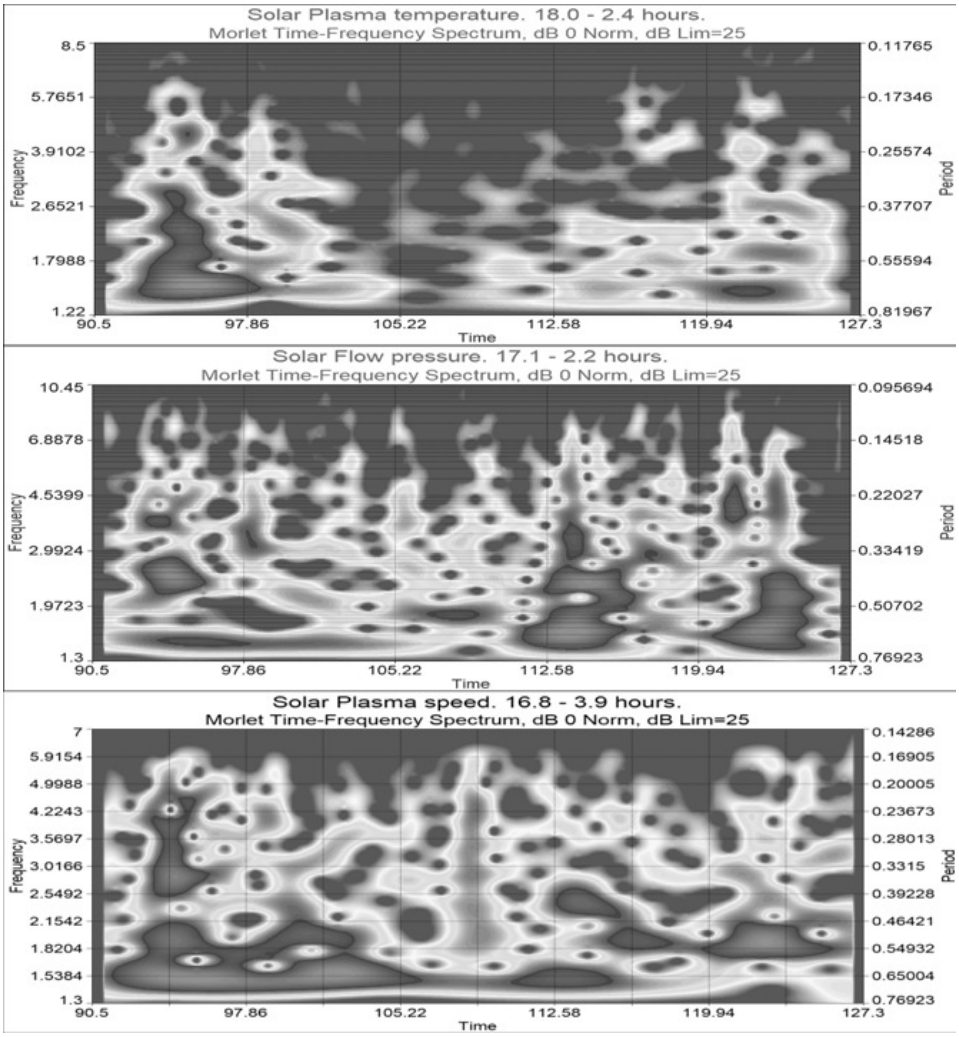


Figure 8 Example of wavelet spectra from data with hourly averaging for temperature (above), pressure (middle) and solar wind speed (below). On the left along the Y axis is frequency in cycles per day, on the right, the period in decimal fractions of day; along the X axis, time in decimal fractions days of year (DOY – day of year). Intensity of wavelet amplitude (Z axis) is shown by gradation of gray (from light-gray to dark-gray). Quasiperiodic components are visible as stripes along the X axis, if they have a incline, then the period changes over time, irregular components are visible as vertical short-time stripes.

suppressing faster low-amplitude variations on digital spectra. Data thus prepared were used to construct wavelet spectra, an example of graphs for solar wind speed is shown in Figure 9.

In all four studied wind parameters, a set of diurnal harmonics appeared, periods of which vary slightly over time. In the above example, for variations in solar wind speed, the main values of quasiperiods are $\approx$ 9.5, 4.5, 2, 1.3 hours, as well as several

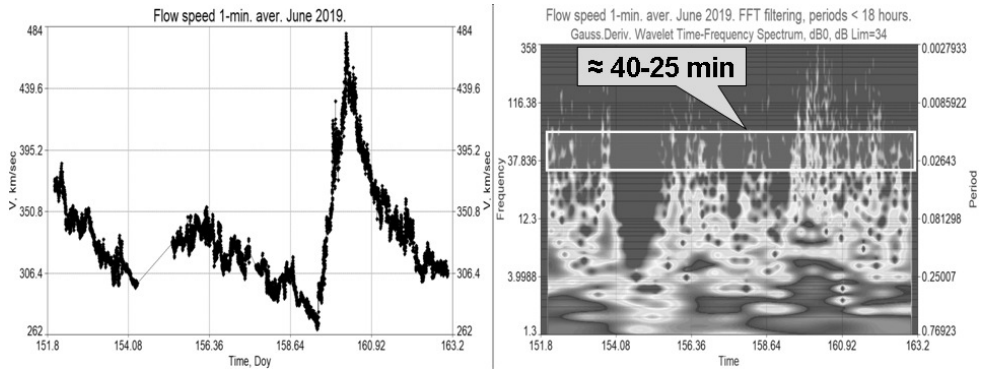


Figure 9 On the left is initial graph of variations in solar wind speed in June 2019 with 1-min averaging, on the right is wavelet spectrum (in dB0, normalized to zero decibels) of filtered time series, with periods shorter than 18 hours. The flag indicates the approximate band of shortest significant quasiregular variations with periods from ≈40 to ≈25 minutes. A sharp impulse increase in wind speed is visible on June 8, 2019.

maxima in periods band 50–40–25 minutes. For the remaining three parameters, the following quasiperiods were obtained: 15.5, 7.5, 6, 3.2, 2, 1.2 hours (for series of proton density); 11.6, 8.5, 6.1, 3.2, 2, 1.4 hours (for series of plasma temperature); 16.3, 6, 2.7, 1.8, 1.3 hours and 44, 35 minutes (for series of pressure in solar wind). To determine the minimum characteristic time of variations, an FFT filter was used, part corresponding to sections of FFT spectra with periods of less than 1 hour was extracted from initial interpolated data. Minimum significant characteristic time of variability on maxima of FFT spectra, at confidence level 99.9% (shows that only one out of thousand sets of random noise can give maximum with height, comparable with height of periodogram maximum) was in the range from ≈25 to ≈15 minutes.

7 Discussion

Observations of flux density variations of galactic radio source 3C 144 (Taurus A) at 1.6 GHz (May) and 5, 6.1 GHz (July) performed in May and July 2019 at the 32-m radio telescope of the Ventspils International Radio Astronomy Center (Latvia) showed a possible connection between the observed variability with disturbances in the solar wind as a result of active events on the Sun. At frequency 1.6 GHz, characteristic variability times in different observation sessions are about 18, 16, 12, 4, 2, 1 hours and shortest, about 20 minutes. At frequencies 5 and 6.1 GHz, characteristic variability times are about 2 hours and 30–40 minutes. Minimum characteristic time of irregular variations at frequencies 5 and 6.1 GHz is about 5–10 minutes. Perhaps this is the appearance of ionospheric effects or external interference. Analysis of fast solar wind variations of parameters (speed, pressure, temperature, particle density) according to data from the NASA OmniWeb catalog, with hourly, 5-minute and 1-minute averaging, showed the following results. In April–May 2019, main quasiperiods of variations in solar wind parameters were in the range from 16 to 5–4 hours (1-hour averaging).

For observations with 5-minute averaging in April–July 2019, a set of main (providing observed dynamics) quasiperiods in approximately the same range, shorter interval of significant quasiperiods in the range of 1–3 hours was added. For observations in June 2019 with 1-min averaging,the range of main quasiperiods expanded from 16 hours to 50–25 minutes. Constructed wavelet spectra showed that these quasiperiods vary slightly over time. Obtained results are in good agreement with quasiperiods in variability of 3C 144 radio source at frequencies 1.6, 5, and 6.1 GHz. This suggests that even at such high frequencies emission from translucent radio source responds to disturbances in solar wind caused by flares, coronal holes and mass ejections occurring on the Sun. This is best seen, most notably at 1.6 GHz. Observations at frequencies 5 and 6.1 GHz showed the presence of quasiperiodic variations in flux, on some days, corresponding to geomagnetic disturbances. Quite a high correlation (0.73) between 5 and 6.1 GHz in left and right circular polarizations and the presence of a weak parabolic trend suggest that data may have its own 3C 144 source variability, which is still not very noticeable due to a short duration of observations. Increase of frequency of obtaining flux density readings up to 3 per second, which was tested on observations in July 2019, showed that, in addition to being able to observe very fast variations in flux density of radio emission, the level of noise and interference increased. Inaccuracies could also occur in pointing the telescope to the source, which sometimes led to sharp and deep falls in flux density. Taking these factors into account will make it possible to further improve the methodology for observing.

The nature of observed variability, which of course is not classical scintillations (since the typical characteristic time of interplanetary scintillations is usually about 1 second), is most likely explained by refraction of radio emission from the Taurus A source, on moving large inhomogeneities of solar wind [18]. A study of the Crab Nebula flux variations in meter wavelength range, with characteristic times of about minutes, tens of minutes and hours, was carried out at the BSA antenna, Pushchino Radio Astronomy Observatory [19]. In this work, it was shown that the observed long-term (compared to interplanetary scintillation) variations of radio emission are not related to the ionosphere and are determined by large-scale disturbances in solar wind and large plasma inhomogeneities, through which 3C144 radio emission passes. However, high-frequency observations of 3C 144 in decimeter and centimeter ranges, with good time resolution, are still quite small. Observations similar to those made at VIRAC were performed at frequencies 403 and 1705 MHz in 1967, and showed wave-like change in flux of the Crab nebula when approaching the Sun, with a trend towards the flux increase, which reached a maximum on June 16–17 [20].

Additionally, analysis of archival observations was made (at frequency 25 MHz) of the 3C 144 radio source for 2003, obtained on the phased array "URAN-4" at the Odessa Observatory of the Radio Astronomy Institute of the National Academy of Sciences of Ukraine. An increase in the level of 3C144 radio source flux is noted at certain phases of increased geomagnetic activity according to the Odessa Observatory. Also, an increase in the speed of solar wind leads to this effect.

An increase in electron concentration in the ionosphere and flows of electrons and protons of solar wind lead to the effect of a decrease of the flux of 3C144 source.

When observing the source at night, the prevailing reaction of 3C144 radio source flux to corpuscular particle flows is noted.

All effects of change in flux of 3C144 radio source are associated with the change

in state of solar wind and ionosphere under the influence of solar and geomagnetic activity.

The nature of reaction to changes in flux of radio source depends onthe time of its culmination and may be different when observing during day and night.

Due to the large amount of observational data from the URAN-4 radio telescope carried out as a result of long-term monitoring fluxes of powerful space radio sources (from 1987 to the present), a detailed study of the appearance of space weather effects in the ionosphere is possible, which will be carried out in subsequent works.

Thus, work performed and analysis of its results show promise of further joint observations of the 3C 144 radio source on VIRAC radio telescopes and decameter low-frequency antenna arrays (UTR-2, URAN, GURT in Ukraine and the LOFAR section in Latvia). This integrated approach allows us to see responses to solar active events, both in the solar wind and in the ionosphere.

8 Conclusions

1. From May 1 to May 21, 2019, while decreasing angular distance between the 3C 144 radio source and the Sun, at frequency 1.6 GHz, there was a small linear trend of increasing flux density from 784 to 834 Jy.

2. On days, when disturbances are observed in solar wind (increase in speed, density, temperature and particle concentration), the amplitude of the 3C 144 variability increases on 1.6 GHz frequency and its characteristic time decreases.

3. Analysis of solar wind parameters with 1-hour, 5-minute and 1-minute averaging for April–May, June and April–July 2019 showed that during the main quasiperiods of variations these parameters are quite close to quasiperiods in variations of the 3C 144 source flux density at frequencies 1.6 GHz and 5, 6.1 GHz.

4. The existence of interconnection between geomagnetic disturbances (according to the Odessa magnetic station data) and change in the 3C 144 flux density from observations at frequency 25 MHz on the low-frequency phased array URAN-4 of the Odessa Observatory of the Radio Astronomy Institute of the NAS of Ukraine is shown. On days when there are magnetic storms and the passage of high-speed solar wind, the flux density of 3C 144 shows a tendency to decrease and increase depending on the phase of appearance of magnetic storms and geomagnetic disturbances.

5. According to observations in July 2019, a high correlation was found between 5 and 6.1 GHz as well as the presence of weak parabolic trends in change in flux density of 3C 144 in left and right circular polarizations. This may indicate a possible contribution of the Crab Nebula's own variability. For a more detailed understanding of this, long-term and regular observations of the 3C 144 source are necessary, which will be continued in future at decimeter and centimeter ranges on VIRAC radio telescopes.

Acknowledgements

The contribution of Artem Sukharev has been funded by ERDF postdoctoral grant No. 1.1.1.2/VIAA/2/18/363 "Investigation of intra-day and inter-day variability of

various types of extragalactic radio sources using telescopes of the Ventspils International Radio Astronomy Centre (RISE)". The project is being implemented in Ventspils University of Applied Sciences.

References

1. Hester J. Jeff. The Crab Nebula: An Astrophysical Chimera. Annual Review of Astronomy & Astrophysics, 2008, Vol. 46, Issue 1, P. 127-155
2. Vitkevich V.V. A new method for studying the solar corona. DAN USSR. 1951, V. 77, P. 34-37
3. Vitkevich V.V. The results of observations of radio wave propagation through the solar corona. Astronomical Journal. 1955, V. 32, P. 106-120
4. Qiang Yuan, Xuefeng Wu, Peng-Fei Yin, Xiao-Jun Bi. A Statistical Model for the γ -ray Variability of the Crab Nebula. The Astrophysical Journal Letters. 2011, Vol. 730, Issue 2, P. L15
5. C. Greiveldinger, B. Aschenbach. Temporal Variability of the X-Ray Emission of the Crab Nebula Torus. 1999, The Astrophysical Journal, Vol. 510, P. 305
6. M. Bleiders, Vl. Bezrukovs, A. Orbidans. Performance Evaluation of Irbene RT-16 Radio Telescope Receiving System. Latvian Journal of Physics and Technical Sciences. 2017, Vol. 54, P. 6
7. V.G. Derevyagin, E.A. Isaeva, R.O. Kravetz, O.A. Litvinenko, S.K. Panishko. Observations of the power cosmic radio sources on the radio telescope URAN-4 during 1998-2004. Astronomical and Astrophysical Transactions. 2005, Vol. 24, No. 5, P. 421-424
8. O.Rioul, P.Duhamel. Fast Algorithms for Discrete and Continuous Wavelet Transforms. IEEE Transactions on Information Theory. 1992, Vol. 38, No. 2, P. 569-586
9. Christopher Torrence, Gilbert P. Compo. A Practical Guide to Wavelet Analysis. Bulletin of the American Meteorological Society. 1998, Vol. 79, P. 61-78
10. Press W.H., Rybicki G.B. Fast algorithm for spectral analysis of unevenly sampled data. Astrophysical Journal. 1989, Vol. 338, Part 1, P. 277-280
11. Fredric J. Harris. On the use of windows for harmonic analysis with the discrete Fourier transform. Proceedings of the IEEE. 1978, Vol. 66, No. 1, P. 51-83
12. Marquardt D. An Algorithm for Least-Squares Estimation of Nonlinear Parameters. SIAM Journal on Applied Mathematics, 1963, Vol. 11, No. 2, P. 431441
13. W.Popinski, W.Kosek. The Fourier transform band pass filter ant its application for polar motion analysis. Artifical Satellites, Planetary Geodesy. 1995, Vol. 30, No. 1, P. 9-25
14. M.I. Ryabov, A.L. Sukharev, M.I. Orlyuk, L.I. Sobitnyak, A.A. Romenets. Comparative Analysis of Geomagnetic Disturbances in The Odessa Magnetic Anomaly Area in The 24th Solar Activity Cycle. Radio phys. radio astron. 2019, Vol. 24, No. 1, P. 68-79
15. A.L. Sukharev, M.I. Orlyuk, M.I. Ryabov, A.A. Romenets. On The First Results of Measurements of Geomagnetic Short-Period Field Variations in The Odesa Magnetic Anomaly Zone with a Second-Long Resolution. Radio phys. radio astron. 2018, Vol. 23, No. 2, P. 116-127

16. Les Piegl, Wayne Tiller. Algorithm for approximate nurbs skinning. Computer-Aided Design. 1996, Vol. 28, Issue 9, P. 699-706
17. H. Akima. A New Method of Interpolation and Smooth Curve Fitting Based on Local Procedures. Journal of the ACM. 1970, Vol. 17, Issue 4, P. 589-602
18. J.T. Gosling. Largescale inhomogeneities in the solar wind of solar origin. Reviews of Geophysics, 1975, Vol. 13, Issue 3, P. 1053-1058
19. V.I. Vlasov. Variations in the cosmic source intensity during radio astronomical studies of the solar wind. Geomagnetism and Aeronomy, 2013, Vol. 53, Issue 2, P. 137-146
20. Larry W. Brown. Three frequency observation of the 1967 Crab Nebula occultation by the Solar Corona. 1969, NASA Goddard Space Flight Center